PHYSICAL REVIEW C VOLUME 44, NUMBER 3 SEPTEMBER 1991

^{14}C photoproton cross section

D. J. McLean, M. N. Thompson, and D. Zubanov
School of Physics, The University of Melbourne, Parkville, Victoria 3052, Australia

K. G. McNeill
Department of Physics, University of Toronto, Toronto, Ontario, Canada M5S 1A7

J. W. Jury
Department of Physics, Trent University, Peterborough, Ontario, Canada K9J 7B8

B. L. Berman
Center for Nuclear Studies, Department of Physics, The George Washington University, Washington, D.C. 20052
(Received 5 November 1990; revised manuscript received 1 July 1991)

The $^{14}C(\gamma,p)^{13}B$ reaction cross section has been measured from threshold to 29.1 MeV using bremsstrahlung photons. A contribution from the $^{14}C(\gamma,pn+d)^{12}B$ reactions is included, and is significant only at the highest energies measured here. The main features of the cross section are a weak resonance at $\approx$22.5 MeV and a dominant, broad resonance at $\approx$25.6 MeV. The integrated cross section up to 29.1 MeV is 17.9 ± 3.2 MeV mb. We deduce that essentially the entire cross section results from decay of $T_>$ dipole states. In combination with the previously reported photoneutron cross section an estimate of the total photoabsorption cross section for ^{14}C is obtained. The $T_<$ and $T_>$ components of the photoabsorption cross section (up to 30 MeV) are estimated to carry strengths of 88 ± 12 MeV mb and 37 ± 8 MeV mb, respectively. An isospin splitting of the giant dipole resonance of 8.4 ± 0.5 MeV is obtained. Comparisons of several shell-model calculations are made with the data, and general agreement is found. A comparison of photoabsorption cross sections for ^{12,13,14}C and ^{16,17,18}O shows dramatic redistribution of dipole strength as neutrons are added to the core nuclei.

I. INTRODUCTION

This paper reports the first measurement of the $^{14}C(\gamma,p)$ cross section. It forms the last of a series of measurements investigating the nuclear photoeffect in light nuclei that consist of a closed shell or subshell coupled to one or two nucleons or holes. The measurements around ^{16}O are now complete, and the following reactions have been measured: the $(\gamma,1n)$ and $(\gamma,2n)$ cross sections for ^{15}N [1–3], ^{17}O [4], and ^{18}O [5,6]; the (γ,n_0) cross section for ^{15}N [7], ^{17}O [8], and ^{18}O [9]; and the (γ,p) cross section for ^{17}O [10], and ^{18}O [5]. The measurement reported here completes the data from the carbon isotopes: the $(\gamma,1n)$ and $(\gamma,2n)$ cross sections for ^{13}C [11], and ^{14}C [12]; the (γ,n_0) cross section for ^{13}C [13] and ^{14}C [14]; and the (γ,p) cross section for ^{13}C [15].

There are relatively few photonuclear data for ^{14}C; the $(\gamma,1n)$ and $(\gamma,2n)$ cross sections have been measured by Pywell *et al.* [12], the (γ,n_0) cross section by Kuo *et al.* [14], and the (n,γ_0) cross section by Wright *et al.* [16]. The (γ,n_{tot}) cross section [sum of $(\gamma,1n)$ and $(\gamma,2n)$ cross sections] shows significant strength around 15 MeV (the so-called "pygmy" resonance) which may be associated with valence-neutron excitations, particularly since the (γ,n_0) cross section accounts for most of the observed strength. The $^{14}C(\gamma,n_{tot})$ cross section is unusual in that the strength in the pygmy region is higher than that in the main giant dipole resonance (GDR) region. Shell-model calculations [17–20] predict that the main GDR strength, which results from core excitations, dominates the photoabsorption cross section. We expect the (γ,p) reaction to provide localized strength in the region of the main GDR, at around 25 to 27 MeV. If this strength is not found, the role of core excitations in the photoabsorption process in ^{14}C must be reexamined.

According to the weak-coupling model [21], the photoabsorption cross section for ^{14}C should contain strength due to single-particle excitations of the two valence neutrons, forming the pygmy resonance, and strength arising from core-nucleon transitions, forming the main strength of the GDR. The observation of the pygmy resonance in the ^{14}C photoneutron cross section [12,14,16] is consistent with these expectations. The $^{14}C(\gamma,p)$ cross section represents core transitions, so that comparison with the $^{12}C(\gamma,p)$ cross section should directly show the effect of the two valence neutrons on the ^{12}C core, and provide a test of the weak-coupling hypothesis for the GDR states.

The nucleus ^{14}C has a ground-state isospin $T_0 = 1$, so that $E1$ excitation can populate states with isospin $T = T_0 = 1$ (the $T_<$ states) and $T = T_0 + 1 = 2$ (the $T_>$ states). The relative strengths and the energy distribution of these isospin components of the GDR have been discussed by several authors [22–26]. Several groups have

made shell-model calculations of the total photoabsorption and partial cross sections, and of the $T_<$ and $T_>$ components of the GDR [17–20]. To test these predictions, it is necessary to identify the isospin components of the photoabsorption cross-section features. This requires knowledge of the various particle decay channels. Together with the ^{14}C photoneutron cross-section data, the present measurement assists in this identification.

II. EXPERIMENT AND ANALYSIS

The $^{14}C(\gamma,p)$ cross section was derived from the yield of induced β^- activity from residual ^{13}B. Activation yield curves were measured as a function of bremsstrahlung tip energy using the University of Melbourne 35-MeV betatron. The ^{13}B nucleus decays 92.1% of the time to the ground state of ^{13}C with a maximum β^- energy of 13.44 MeV and a half-life of 17.4 ms [27]. The $^{14}C(\gamma,d)$ and $^{14}C(\gamma,pn)$ reactions lead to residual ^{12}B, which is also a β^- emitter, with a half-life of 20.4 ms and an end-point energy of 13.37 MeV, decaying 97.1% of the time to the ground state of ^{12}C [28]. Decays of ^{12}B could not be distinguished from those of ^{13}B, so that above the (γ,d) and (γ,pn) thresholds (23.49 and 25.71 MeV, respectively), the reported cross section is that for the $^{14}C(\gamma,p+pn+d)$ reactions. The high end-point energy of the β^- spectra allowed detection of the activity using NaI detectors in the experimental arrangement described below and shown in Fig. 1.

The sample consisted of 7.8 ± 0.2 g of ^{14}C (and 1.5 ± 0.1 g of ^{12}C impurity) in the form of enriched elemental carbon powder, encapsulated in two rectangular containers of size $48 \times 50 \times 6$ mm^3 with 0.0025-mm-thick copper walls. The two containers were separated by 48 cm and placed at an angle of 45° to the incident beam direction, as shown in Fig. 1. Each container was observed by two large NaI detectors 6.3 cm from the beam axis, placed so that the detector face was perpendicular to the beam direction. The two detectors associated with the upstream target were positioned in a horizontal plane, while those associated with the downstream sample were in a vertical plane. Shielding was arranged to ensure that the two detector systems were independent. The reasons for the use of two samples and separate detector systems will be discussed below.

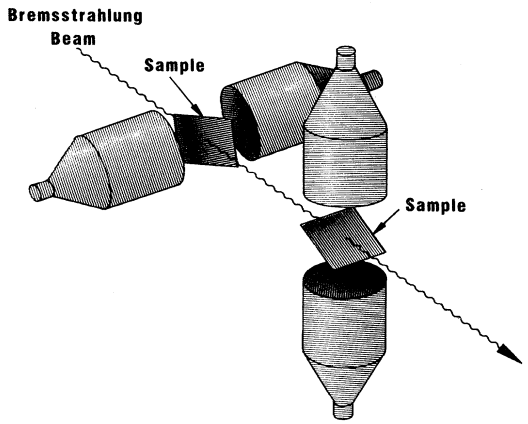

FIG. 1. Experimental arrangement of the samples and detectors.

Each detector was surrounded by up to 2 mm of cadmium to attenuate background resulting from thermal neutron activation. The cadmium shielding was also placed on the front face of each detector to attenuate the intense flux of bremsstrahlung photons produced in the sample by electrons from the β^- decay of ^{14}C ($Q_{\beta-} = 157$ keV) [27]. Photomultiplier-tube pileup was thereby reduced to acceptable levels. General shielding around the detectors was provided by 20 cm of steel.

The activity was induced during the 50 Hz, 2-μs-long beam burst from the betatron, and counted for a period of 12 ms starting 4 ms after each beam burst. The photomultiplier tubes were electronically desensitized during the beam burst to maintain their stability. Long term gain stability was further improved by using analog gain stabilizers. These stabilizers were referenced to a peak in the spectrum of weak ^{60}Co sources, which were situated near each pair of detectors. These sources, and weak ^{88}Y sources, also provided a means of calibrating each spectrum.

The bremsstrahlung beam was collimated to a diameter of 33 mm at the position of the downstream target. The bremsstrahlung flux was measured using a thin-walled transmission ion chamber, placed upstream of the samples. This chamber was intercalibrated against a replica P2 ionization chamber [29].

At each betatron energy, a pulse-height spectrum was accumulated from each detector, and recorded together with the measured flux and the system live time. The recorded β^- spectra were integrated over an energy range of 3.7 to 11.5 MeV; a lower limit of 3.7 MeV was chosen to eliminate background arising from long-lived activity induced in the NaI crystals by thermal neutrons, and to minimize other low-energy machine-induced background.

Nineteen independent yield curves were measured at bremsstrahlung tip energies ranging from 20.7 to 29.5 MeV in 100-keV intervals. Each curve took about nine hours to complete, and was done under computer control of beam parameters. A reference yield point was taken at a standard energy (27 MeV) after every ten points, as a check of reproducibility.

Several measurements were made to determine the magnitude of potential sources of background. The room and cosmic-ray background, measured carefully, accounted for 17% of the detected activity at 28 MeV. Measurements were made of the yield with no sample in the beam, and were found to be negligible. Further yield measurements were made using a sample of ^{12}C graphite and copper foil that was twenty times the thickness of these materials present within the ^{14}C target. These measurements determined that the contribution from the ^{12}C impurity and the casing to the measured ^{14}C target yield was small ($\approx$1% at 25 MeV and $\approx$0.5% at 28 MeV). Furthermore, since this yield was zero below 21 MeV, it was concluded that background contribution due to beam scattering from the sample was negligible.

At energies below the photoproton reaction threshold of 20.83 MeV, the measured ^{14}C-sample yield was nonzero, indicating a significant source of background due to the ^{14}C sample itself. This background originated from activation of the detectors by neutrons produced in the sample via the $^{14}C(\gamma,n)$ reaction, for which the threshold is relatively low (8.18 MeV). This background photoneutron yield was derived as a function of bremsstrahlung tip energy from the $^{14}C(\gamma,n)$ cross section of Pywell *et al.* [12], and normalized to the yield measured in this experiment below the $^{14}C(\gamma,p)$ reaction threshold. This estimated background, amounting to $\lesssim$19% of the ^{14}C-sample yield at 25 MeV and $\lesssim$4% at 28 MeV, was subtracted from the measured ^{14}C-sample yield.

An aberration of the University of Melbourne betatron produced a small energy-dependent shift in the direction of the bremsstrahlung beam. At high energies, photographs showed that the most intense region of the beam shifted at most by 3 mm. This shift produced changes in the solid angle subtended at the active region of the target by opposing detectors. A shift in the beam position would also result in a different average path length, and hence average energy loss, for β^- particles within the sample. This would affect the number of particles exiting the target, and distort the yield measurement. The detector geometry described above, and in particular the use of thin samples placed at 45° to the beam, minimized the effects of beam shift. These effects were further reduced by normalizing the yield curves from each detector system to a common relative efficiency and then averaging the yields of opposing detectors. The yield-curve shapes determined separately for the horizontal and vertical detector systems were in good agreement, except above 28 MeV where they differed by up to 4%. This discrepancy could not be resolved, and so after normalizing the horizontal detector-system yield curve to that from the vertical (for which we determined the absolute efficiency), the average of the yields from the two systems was taken for further analysis. The final yield curve may be in error by up to ±2% in the region above 28 MeV.

The absolute detection efficiency was determined by measuring the activation yield for the $^{13}C(\gamma,p)^{12}$B reaction. We assumed that the shapes of the ^{12}B and ^{13}B β spectra are nearly identical, and hence that the difference in the detection efficiencies of ^{12}B and ^{13}B activity was negligible. This assumption was justified in view of the near-equality of the half-lives, Q_{β^-}, and $\log ft$ values of the ^{12,13}B decays [27,28]. The measured activation yield was normalized to that used by Zubanov *et al.* [15] in deriving their $^{13}C(\gamma,p)^{12}$B cross section, also measured in this laboratory. We used a 5.062-g sample of ^{13}C graphite powder (with a 0.323-g ^{12}C impurity), encapsulated in a rectangular container identical to those of the ^{14}C samples for this normalization. This sample was irradiated in the same position as occupied by the downstream ^{14}C sample. Seven yield curves were measured with bremsstrahlung tip energies ranging from 17.0 to 29.5 MeV in 0.5-MeV intervals. The yields from the two opposing detectors were averaged, and a small contribution from the ^{12}C impurity was subtracted. The resulting yield-curve shape was found to match precisely that obtained in the earlier measurement [15] made in this laboratory.

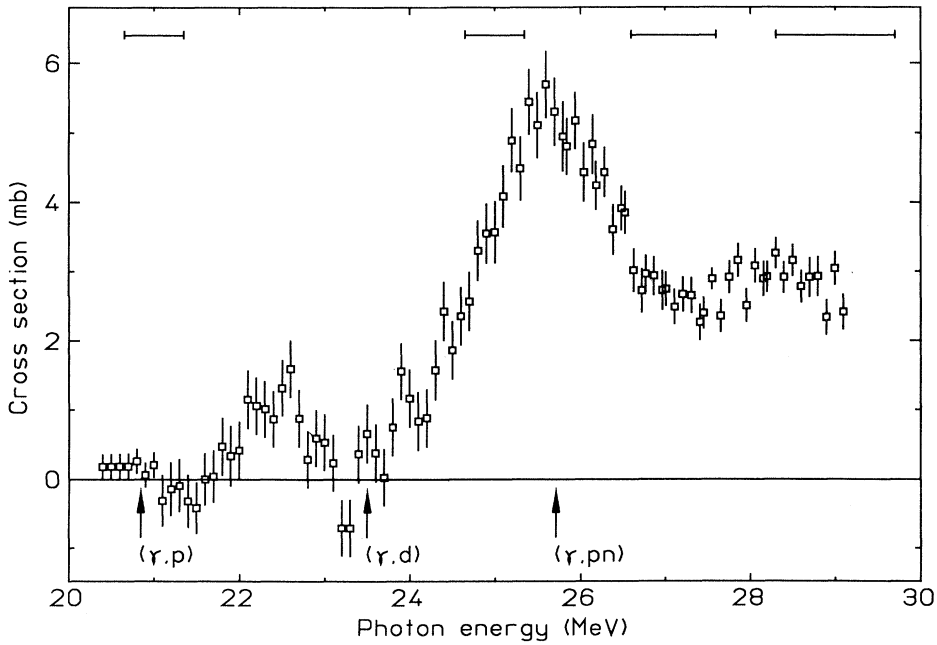

FIG. 2. The $^{14}C(\gamma,p+pn+d)$ reaction cross section. The horizontal bars represent the bin widths used in the analysis and indicate the energy resolution of the data. The error bars on the data points represent statistical uncertainties only; there is an additional systematic uncertainty of ±16% in the absolute cross-section scale.

The absolute yield was analyzed using the variable-bin Penfold-Leiss method [30] to produce the cross section shown in Fig. 2. The cross section around 28 MeV may be in error by up to ±0.7 mb, due to the uncertainty in the yield in the region above 28 MeV (see above). In addition to the statistical uncertainties in the cross section, there is a systematic uncertainty of ±16% in the absolute scale. This arises from an uncertainty of ±13% in the absolute scale of the $^{13}C(\gamma,p)$ cross section of Zubanov *et al.*, the uncertainty of ±2% in the mass of the ^{14}C sample, and a statistical uncertainty of ≈ ±1% in the normalization of the $^{13}C(\gamma,p)^{12}B$ activation yield measured here to that of Zubanov *et al.* The energy calibration was determined by observation of breaks in several well-known photoneutron yields. The energy scale has an uncertainty of ±50 keV at 21 MeV, increasing to ±200 keV at 29 MeV.

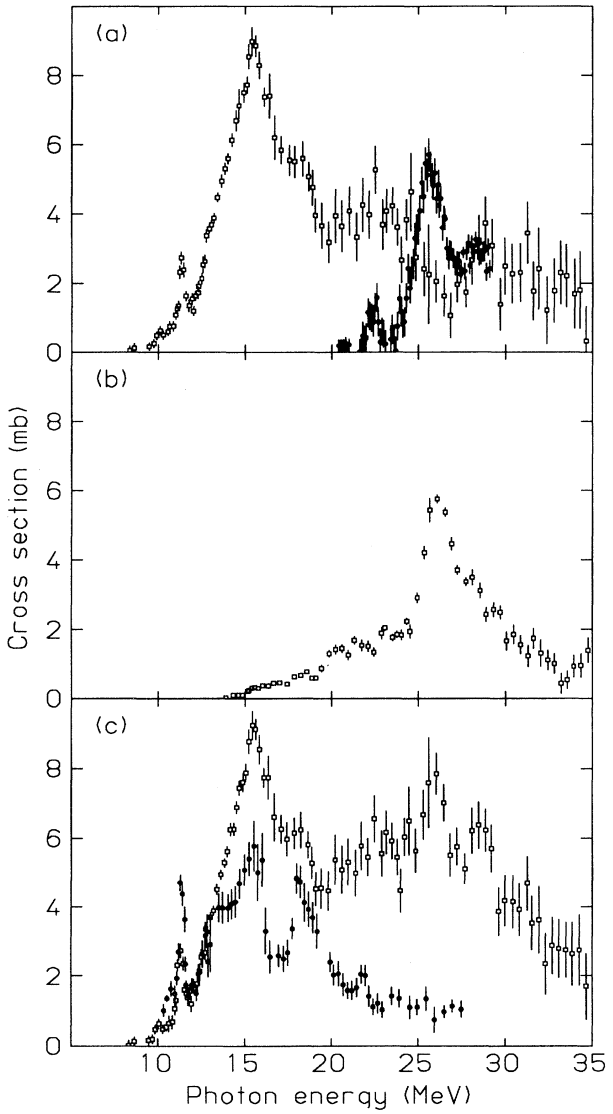

FIG. 3. Photonuclear cross section data for ^{14}C: (a) $\sigma(\gamma,p+pn+d)$ [present work] (solid circles) and $\sigma(\gamma,1n)$ [12] (open squares); (b) $\sigma(\gamma,2n)$ [12]; and (c) $\sigma(\gamma,n_{tot}) = \sigma(\gamma,1n)+\sigma(\gamma,2n)$ [12] (open squares) and $\sigma(\gamma,n_0)$ [14] (solid circles).

III. RESULTS AND DISCUSSION

A. Cross section

The $^{14}C(\gamma,p)^{13}B$ cross section is shown in Fig. 2; it includes the contribution from the $^{14}C(\gamma,pn+d)^{12}B$ reactions. The present cross section is compared with the available photonuclear data in Fig. 3. Figure 4 shows the energetics of ^{14}C photoreactions; various reaction thresholds and relevant states are indicated.

The present cross section features a peak at ≈22.5 MeV, and the dominant structure centered at ≈25.6 MeV. Significant strength continues above 27 MeV with evidence of a broad structure centered at ≈28 MeV. The dominant structure at 25.6 MeV is also seen in the $(\gamma,2n)$ cross section. In this energy region a substantial dip is evident in the $^{14}C(\gamma,1n)$ cross section.

It should be noted that strength from the (γ,pn) reaction channels is included in both the photoproton and the $(\gamma,1n)$ cross sections. We can obtain an estimate of this contribution, for which the difference of the $(\gamma,1n)$ and (γ,n_0) cross sections is an upper limit. In the region of the (γ,pn) threshold (25.71 MeV), the $(\gamma,1n)$ cross section is dominated by strength from the (γ,n_0) reaction. As the $(\gamma,1n)$ cross section rises above the (γ,pn) threshold, the average single-neutron energy falls, and then remains low [12], indicating that high-lying states in ^{13}C are populated preferentially. The low average neutron energy suggests that the other open channels [$(\gamma,n\alpha)$ and (γ,nd)] do not make a significant contribution to the $(\gamma,1n)$ cross section in this region, and that the observed rise in the $(\gamma,1n)$ cross section may be associated with the (γ,pn) reaction. Then, the difference between the $(\gamma,1n)$ and (γ,n_0) cross sections is a fair estimate of

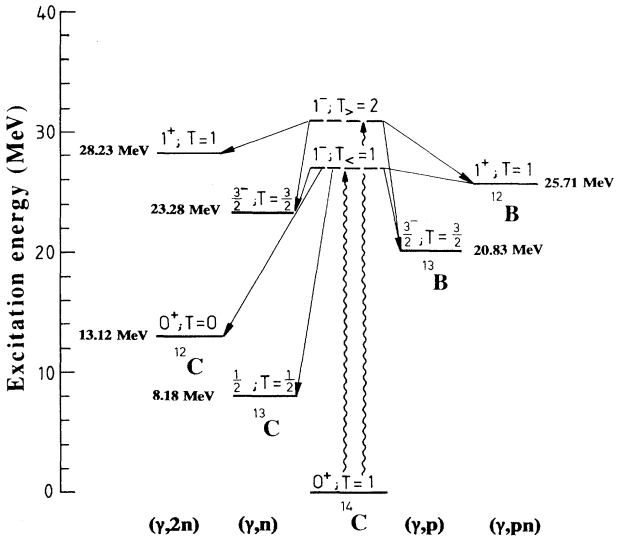

FIG. 4. Energetics of photoreactions in ^{14}C.

the (γ,pn) cross section. This estimate yields a (γ,pn) cross section of $\approx$2.5 mb at 28 MeV, which would account for the strength above 27 MeV and the broad structure at $\approx$28 MeV in the present work. There are no data for the ^{14}C(γ,d) reaction, but we expect the cross section to be small [31,32].

The strength from the (γ,p) reaction represents transitions almost entirely from the ^{12}C core. Electric dipole excitation of protons from the core will form only 3p–1h states of $J^\pi;T=1^-;(1,2)$ and configuration $(\pi p_{3/2})^{-1}(\pi 2s\text{–}1d)^1(\nu p_{1/2})^2$. We then expect only a few major transitions to contribute to the cross section. The observation of only a few structures in the present cross section is consistent with this expectation.

Comparison of the photoproton cross section with the $(\gamma,1n)$ and $(\gamma,2n)$ cross sections of Pywell *et al.* [12] and the (γ,n_0) cross section of Kuo *et al.* [14] may allow determination of the isospin character of the features observed in the present cross section. These assignments are discussed below.

1. The structure at 22.5 MeV

The 22.5-MeV resonance observed in the present measurement is reported here for the first time [27]. There is no clear evidence of a peak at 22.5 MeV in the $(\gamma,1n)$ and $(\gamma,2n)$ cross sections of Pywell *et al.* [12], nor in the $T_<$-selective (γ,n_0) cross section of Kuo *et al.* [14] (see Fig. 3). The bump evident in the (γ,n_0) cross section at $\approx$21.9 MeV is too low in energy to correspond to the feature observed in the present work. The location of this bump is possibly even lower than observed by Kuo *et al.*; their energy calibration seems to require a shift towards lower energies to match the structure in the (γ,n_0) cross section derived by detailed balance from the ^{13}C(n,γ_0) cross section of Wright *et al.* [16] (see Fig. 3 of Ref. [14]).

This resonance occurs well below the (γ,d) and (γ,pn) thresholds, implying that it belongs to the (γ,p) cross section. Energetically, only the $T=\frac{3}{2}$ ground state of ^{13}B is accessible for proton decay of this resonance, whereas neutron decay is possible to the many $T=\frac{1}{2}$ states accessible in ^{13}C (see Fig. 4). If this resonance had a $T=1$ character, neutron decay would be favored over proton decay by the larger number of open channels and the higher penetrability of these channels. Consequently, this structure would be evident in the photoneutron cross section. If the resonance had a $T=2$ character, neutron decay to any of the energetically accessible states in ^{13}C would be isospin forbidden; isospin-allowed neutron-decay channels open at 23.29 MeV with the opening of the first $T=\frac{3}{2}$ state at 15.11 MeV in ^{13}C (see Fig. 4). The photoproton channel would then represent the only isospin-allowed mode for decay of a $T=2$ state in ^{14}C at this energy. Given that this structure is evident in only the photoproton cross section, an assignment of $T=2$ is favored.

2. The main structure at about 25.6 MeV

The dominant feature of the (γ,p) cross section is a broad ($\approx$2 MeV) resonance centered at $\approx$25.6 MeV. If this resonance had a $T=1$ character, then neutron decay would be favored over proton decay; the number of $T=\frac{1}{2}$ states available in ^{13}C is far greater than is available for proton decay (the ground and first excited states of ^{13}B), and the penetrabilities for neutron emission are greater. However, if this resonance had a $T=2$ character, then neutron decay would be isospin forbidden to all states in ^{13}C except the lowest $T=\frac{3}{2}$ state at 15.11 MeV (23.29 MeV excitation in ^{14}C). This state is neutron unstable, and decays strongly to states in ^{12}C (Ref. [27]). Consequently, the transition strength to this state would appear in the $(\gamma,2n)$ cross section rather than the $(\gamma,1n)$. The absence of this major peak in the $(\gamma,1n)$ and (γ,n_0) cross sections and its presence in the $(\gamma,2n)$ cross section (see Fig. 3) is consistent with an isospin assignment of $T=2$. Furthermore, the sharp rise of the $(\gamma,2n)$ cross section at $\approx$24 MeV is consistent with the opening of the 15.11-MeV state in ^{13}C.

3. Structure above 27 MeV

The high-energy region of the present cross section appears to be dominated by strength from the (γ,pn) reaction channels (see above). Although the (γ,pn) reaction can carry both $T=1$ and $T=2$ strength, comparison of the (γ,pn) and $(\gamma,2n)$ cross sections suggests dominant $T=2$ strength. The (γ,np) channels represent the first isospin-allowed modes for sequential two-nucleon decay of $T=2$ states in ^{14}C; isospin-allowed decay of $T=2$ states via the $(\gamma,2n)$ reaction only becomes available at 28.3 MeV with the opening of the 15.10-MeV $T=1$ state in ^{12}C. Above the (γ,pn) reaction threshold (25.71 MeV), the (γ,pn) cross section rises suddenly while the $(\gamma,2n)$ cross section falls sharply. This observation is consistent with an isospin assignment of $T=2$.

B. Integrated cross section

The ^{14}C$(\gamma,p+pn+d)$ cross section integrated to 29.1 MeV (the upper limit of the present measurement) is 17.9 ± 3.2 MeV mb. Extrapolation to 30 MeV yields 21 ± 4 MeV mb, which is to be compared with the strength of 108 ± 11 MeV mb obtained from the $(\gamma,n_{\rm tot})$ cross section of Pywell *et al.* [12]. The sum of these includes the (γ,pn) reaction contribution twice; the integrated strength (to 30 MeV) of the (γ,pn) cross section estimated above is 4 MeV mb. Subtraction of this strength from the above sum yields a good estimate of the total photoabsorption cross-section strength for ^{14}C of 125^{+19}_{-15} MeV mb. This estimate represents strength from all the major reaction channels but excludes strength from the (γ,α) and $(\gamma,^3\mathrm{H})$ channels, the only other open channels below 30 MeV, which may be expected to individually contribute no more than a few percent of the total absorption strength [32].

Table I presents the integrated cross sections (to 30 MeV) for ^{12,13,14}C, ^{14,15}N, and ^{16,17,18}O. The integrated photoproton cross section for ^{14}C is smaller than that for ^{12,13}C and is consistent with the systematic trends noted previously, i.e., with increasing neutron ex-

TABLE I. Integrated photonuclear cross sections (to 30 MeV) for the carbon, nitrogen, and oxygen isotopes.

Nucleus	$\int \sigma(\gamma, n_{tot})\, dE_\gamma$ (MeV mb)	(TRK units)	$\int \sigma(\gamma, p)\, dE_\gamma$ (MeV mb)	(TRK units)	Sum (TRK units)
^{12}C	43[a]	0.24	72[a]	0.40	0.64
^{13}C	96[b]	0.50	42[c]	0.22	0.71
^{14}C	108[d]	0.53	17[e]	0.08	0.61
^{14}N	113[a]	0.54	25[a]	0.12	0.66
^{15}N	92[f]	0.41	70[g]	0.31	0.72
^{16}O	58[a]	0.24	105[a]	0.44	0.68
^{17}O	96[h]	0.38	22[i]	0.09	0.46
^{18}O	143[j]	0.54	31[j]	0.12	0.65

[a]Reference [32].
[b]Reference [11].
[c]Reference [15] (extrapolated from 28 MeV).
[d]Reference [12].
[e]Present data (extrapolated from 29.1 MeV); an estimated contribution (see text) of 4 MeV mb from the (γ, pn) reaction has been subtracted. The (γ, d) cross-section strength is neglected.
[f]Reference [1].
[g]Reference [36].
[h]Reference [4].
[i]Reference [10].
[j]Reference [5].

cess the strength carried by photoneutron channels increases while that carried by photoproton channels decreases, thereby maintaining a nearly constant total absorption strength. The integrated photoabsorption cross section for ^{14}C (to 30 MeV) exhausts 61% of the Thomas-Reiche-Kuhn (TRK) sum. This compares well with those for the neighboring nuclei.

C. Isospin distributions

The relative strengths and the energy distributions of the isospin components of the GDR have been discussed by a number of authors [22–26]. Akyüz and Fallieros [24] give for the separations of the mean energies of the isospin components of the GDR

$$\bar{E}_> - \bar{E}_< = U(T_0 + 1)/A, \tag{1}$$

where the symmetry potential $U = 60$ MeV, and where the mean energy $\bar{E}$ is defined by Leonardi [33] as

$$\bar{E} \equiv \frac{\sigma_0}{\sigma_{-1}}, \tag{2}$$

where

$$\sigma_0 \equiv \int \sigma\, dE \quad \text{and} \quad \sigma_{-1} \equiv \int (\sigma/E)\, dE. \tag{3}$$

For ^{14}C ($T_0 = 1$) this expression gives a separation energy of 8.6 MeV. Fallieros and Goulard [25] and Hayward *et al.* [26] have derived expressions for the relative strengths of the $T_<$ and $T_>$ components. These can be expressed in terms of the ratio of the energy-weighted integrated cross sections $\sigma^{>}_{-1}/\sigma_{-1}$. For ^{14}C, Fallieros and Goulard predict a ratio of 0.37 and Hayward *et al.* predict a similar value of 0.32.

We estimate the two components of the $(\gamma$,tot) cross section as follows. On the basis of the mass of ^{14}B, the lowest $T = 2$ state in ^{14}C lies at 22.5 MeV. Hence we take all the strength in the $(\gamma$,tot) cross section below 22.5 MeV to be $T_<$. Above this energy, we have deduced above that essentially the entire strength in the present cross section, i.e., (γ, p) and (γ, pn), is $T_>$ [the (γ, d) strength, which is $T_<$, is neglected], and have identified the main peak at 26 MeV in the $(\gamma, 2n)$ cross section as $T_>$. Significant $T_<$ strength, however, is present in the $(\gamma, 2n)$ cross section. All the strength in the $(\gamma, 2n)$ cross section up to 23.3 MeV (corresponding to the opening of the first $T = \frac{3}{2}$ level in ^{13}C) is $T_<$. The $(\gamma, 2n)$ cross section at 23.3 MeV is $\approx$2 mb, and it is reasonable to assume that this $T_<$ strength extends to higher energies, providing underlying strength to the main peak at 26 MeV. We have assumed that the $T_<$ component of the $(\gamma, 2n)$ cross section above 23.3 MeV is represented by a Gaussian of width 3 MeV centered at 23.3 MeV, and matching the $(\gamma, 2n)$ cross section at that energy. The range of uncertainty of this $T_<$ component has been estimated by varying the width of the Gaussian from 1.5 to 6 MeV. It should be noted that all the $T_>$ strength present in the $(\gamma, 1n)$ cross section (up to 30 MeV) is carried by the (γ, pn) reaction; all the other open channels [(γ, n), $(\gamma, n\alpha)$, and (γ, nd)] are $T_<$ selective. Uncertainties in the present analysis arise from the estimates of the (γ, pn) cross section and the underlying $T_<$ strength

in the $(\gamma, 2n)$ cross section.

Our estimate of the $T_>$ component of the ^{14}C GDR is shown in Fig. 5(a) and represents the sum of the cross section obtained in the present experiment and the $T_>$ part of the $(\gamma, 2n)$ cross section. The $T_<$ component, also shown in Fig. 5(a), is the difference between the estimated (γ,tot) cross section and the $T_>$ component.

Properties of the estimated isospin components (extrapolated to 30 MeV) are given in Table II. An isospin splitting of 8.4 ± 0.5 MeV is obtained, which compares well with the value of 8.6 MeV obtained from Eq. (1). Akyüz and Fallieros [24] use a symmetry potential U, modified for a collection of dipole states, of 60 MeV. Leonardi [33] suggests smaller values of U for light nuclei. It is interesting to note that estimates of isospin splitting in ^{15}N [2] and ^{17}O [10] support a value of U smaller than 60 MeV, whereas those for ^{13}C [15], ^{14}C, and ^{18}O [5] support a value of U close to 60 MeV.

The ratio $\sigma^{>}_{-1}/\sigma_{-1}$ derived from the present data is 0.22 ± 0.05. Although this ratio is obtained from distributions estimated up to 30 MeV, we do not expect that the strength at higher energies will significantly affect

TABLE II. Some properties of the $T_<$ and $T_>$ distributions (up to 30 MeV). The uncertainties are estimated by considering the uncertainties in the absolute scales of the photoneutron and photoproton cross sections (±10% and ±16%, respectively), in addition to a range of acceptance of $T_<$ and $T_>$ strength discussed in the text.

	$T_<$	$T_>$
σ_0 (MeV mb)	88 ± 12	37 ± 8
σ_{-1} (mb)	4.81 ± 0.60	1.38 ± 0.29
$\bar{E}$ (MeV)	18.3 ± 0.4	26.7 ± 0.1

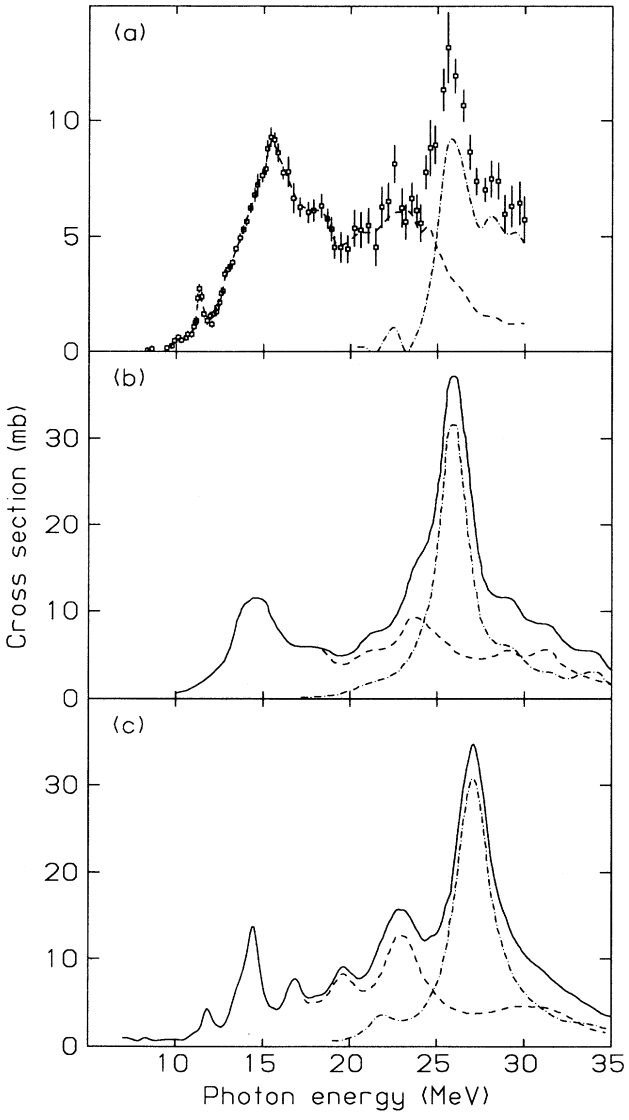

FIG. 5. The total absorption cross section for ^{14}C (data points/solid curve) and its $T_<$ (dashed curve) and $T_>$ (dash-dotted curve) components obtained from (a) present estimate derived from the available photonuclear data, (b) a calculation by Kissener *et al.* [18], and (c) a calculation by Assafiri and Morrison [19].

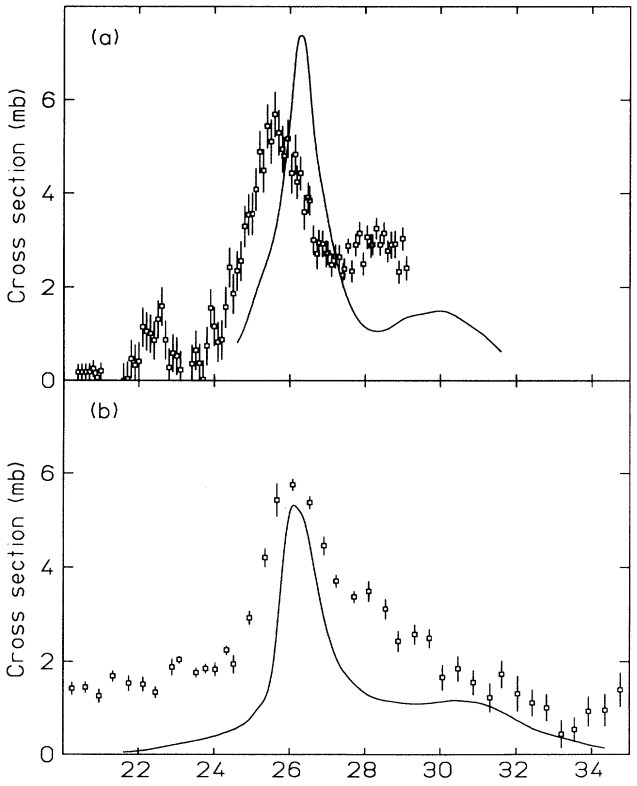

FIG. 6. Comparisons of (a) the present $^{14}C(\gamma, p+pn+d)$ cross section with the $^{14}C(\gamma, p_0)$ cross section calculated by Goncharova *et al.* [20], and (b) the $^{14}C(\gamma, 2n)$ cross section [12] with the $^{14}C(\gamma, n_{15.11})^{13}C$ cross section calculated by Goncharova *et al.* [20].

this value. This value is in poor agreement with the predictions of Fallieros and Goulard [25] and Hayward *et al.* [26] of 0.37 and 0.32, respectively. Both of these model predictions take nuclear dynamic effects into account, although several approximations are made in calculating these. The predictions depend on the isovector radius, which is a function of the neutron and proton rms radii. It is assumed that the proton and neutron rms radii are the same. For ^{14}C, where the neutron excess is relatively large, this assumption is likely to break down. The neutron radius of ^{14}C is unknown [27], but in the case of ^{18}O the neutron radius exceeds the proton radius by 5% [34]. The ^{14}C neutron radius would have to exceed the proton radius by $\approx$8% to bring the prediction of Hayward *et al.* into agreement with the value derived from the present data.

D. Comparison with theory

In recent years several groups have made shell-model calculations [17-20] of the ^{14}C photoabsorption cross section and the distribution of strength between the $T_<$ and $T_>$ isospin components. The calculations share the same basis (and use similar single-particle energies) and differ mainly in the form of residual nucleon-nucleon interactions used. All predict significant $T_<$ strength near 15 MeV and a large amount of $T_<$ strength spread throughout the GDR region, in agreement with our deduced $T_<$ distribution, but all appear to concentrate more $T_>$ strength in the main GDR than is observed.

The calculation by Vergados [17], using the Kuo-Brown interaction, places the dominant $T_>$ strength at $\approx$23.5 MeV, several MeV lower than the observed GDR.

Kissener *et al.* [18], in a calculation using the Cohen-Kurath and Gillet's CAL interactions, predict the dominant $T_>$ component near 26 MeV. Their results are shown in Fig. 5(b) and can be compared with the present photoabsorption cross section and isospin components; there is good agreement in shape and strength distribution. However, the calculation predicts no counterpart to the $T_>$ state seen at 22.5 MeV in the present data.

The calculation of Assafiri and Morrison [19], using the residual interaction of Cooper and Eisenberg, is also in good agreement with the data [see Fig. 5(c)]. It places the main $T_>$ component near 27 MeV. It also predicts a $T_>$ state near 22 MeV that may be the shell-model counterpart to the resonance seen in the present data at 22.5 MeV: the predicted and observed states correspond in excitation energy; they carry a similar fraction of the total $T_>$ strength (5% and 3%, respectively); and they both lie several MeV below the main $T_>$ strength. The main difference between the calculation of Assafiri and Morrison [19] and that of Kissener *et al.* [18] is in the form of residual nucleon-nucleon interaction used. The interaction of Cooper and Eisenberg includes the isospin-exchange term, whereas the Cohen-Kurath and Gillet's CAL interactions do not.

Goncharova *et al.* [20] extended the earlier work of Kissener *et al.* [18] to calculate partial neutron-decay cross sections to the ground state and several excited states in ^{13}C, and the proton-decay cross section to the ^{13}B ground state. As discussed above, the dominant resonance at 25.6 MeV can decay to the ^{13}B ground state, or to the neutron-unstable 15.11-MeV state in ^{13}C, so that the resonance strength is shared between the (γ,p) and $(\gamma,2n)$ channels. The $(\gamma,2n)$ channels also carry significant strength from the decay of $T_<$ states in ^{14}C, and this underlies the structure at 25.6 MeV. Figure 6 compares the calculated ^{14}C$(\gamma,p_0)^{13}$B and ^{14}C$(\gamma,n_{15.11})^{13}$C cross sections with the ^{14}C photoproton and ^{14}C$(\gamma,2n)$ cross-section data. We see that the calculations are in good agreement with the observed branching of the major $T_>$ strength.

E. Systematic trends

We may now make some general comments on the effects, on the $E1$ strength, of adding one or two neutrons to the assumed semi-closed-core ^{12}C and closed-core ^{16}O nuclei. The data presented in Table I show that as neutrons are added to a ^{12}C or ^{16}O core (or proton holes added to a ^{16}O core), the integrated photoneutron cross section increases markedly, its strength more than doubling with the addition of two particles or holes. Conversely the integrated photoproton cross section decreases sharply, by more than a factor of two. As noted above, the fraction of the TRK sum exhausted by the total absorption cross section integrated to 30 MeV is relatively constant.

Figure 7 shows the photoproton, photoneutron, and total absorption cross sections for the carbon and oxygen isotopes. The spreading of the $E1$ absorption strength with increasing neutron number is clearly seen, together with the changes in the distribution of this strength between the two major decay channels.

The addition of a single neutron to a core of ^{12}C or ^{16}O leads to the formation of a smaller resonance (the pygmy resonance) below the main GDR. This strength can be associated with valence-neutron excitations, which are $T_<$ in nature. This is supported by the observation that the pygmy strength in ^{13}C is accounted for by neutron decay to the ground and first excited states of ^{12}C [5], and in ^{17}O by neutron decay to the ground state of ^{16}O [8]. The gross features of the main GDR strength, i.e., its shape, width, and location, have not changed significantly. These observations are generally consistent with predictions of the weak-coupling model [21]. However, a small change in the location of the main GDR strength is observed and is discussed below. Furthermore, a resonance at 20.7 MeV in ^{13}C (assigned $T_<$) [15] has been formed possibly by fragmentation of transition strength from the ^{12}C core by the valence $1p_{1/2}$ neutron.

The addition of two neutrons to the ^{12}C or ^{16}O core changes the cross-section distribution more significantly. The ^{14}C and ^{18}O nuclei show a greatly enhanced strength in the region of the pygmy resonance. The cross-section

strength in the low-energy region is much greater than is expected from a weak-coupling model. In addition, in the case of ^{18}O the main GDR strength seems more disrupted, again not expected on the basis of the weak-coupling picture; the present measurement shows that the main GDR features in ^{14}C are disrupted less than they are in ^{18}O. These observations suggest that unlike the addition of a single neutron (as for ^{13}C and ^{17}O) the addition of two valence neutrons has significantly perturbed the core.

The total absorption cross sections for the carbon isotopes show that the energy at which the major dipole strength occurs increases from 22 MeV for ^{12}C to 24 MeV for ^{13}C and to 25.6 MeV for ^{14}C. It is possible that the energies of the $p_{3/2} \rightarrow (2s\text{–}1d)$ transitions that are mainly responsible for this absorption strength increase with isotope number as a result of changes in ground-state deformation. For the oxygen isotopes, such deformation changes have been linked with systematic trends in the GDR structure [10]. For the carbon isotopes, Mairle and Wagner [35] show that $p_{3/2}$-shell closure is consolidated at the expense of $p_{1/2}$-shell occupancy as the neutron number increases. This decrease in $p_{1/2}$-shell occupancy, from 0.7 in ^{12}C to 0.4 in ^{13}C and to 0.3 in ^{14}C, is linked to decreasing nuclear deformation from a value of $\delta = -0.3$ for ^{12}C to -0.1 for ^{14}C. Consideration of the dependence of the nondegenerate Nilsson levels on deformation shows the energies of the $p_{1/2} \rightarrow (2s\text{–}1d)$ transitions increase from ^{12}C to ^{14}C, as does the energy of the main GDR strength.

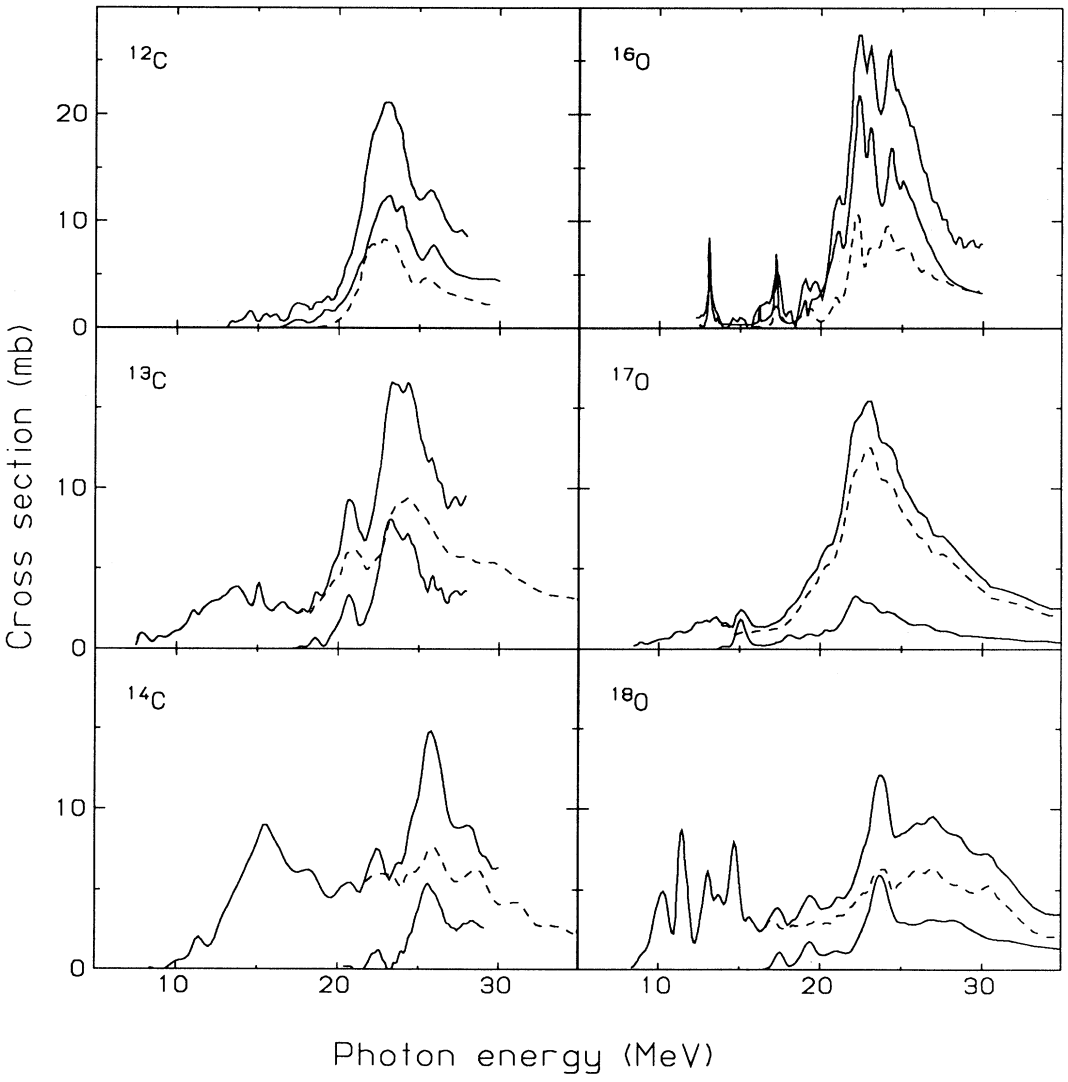

FIG. 7. Comparison of the photoneutron (dashed curve), photoproton (solid curve), and total photoabsorption (solid curve) cross sections for the carbon and oxygen isotopes. The cross sections for ^{12}C and ^{16}O are taken from an evaluation of Fuller [32]. The photoneutron data sources are ^{13}C, Ref. [11]; ^{14}C, Ref. [12]; ^{17}O, Ref. [4]; ^{18}O, Ref. [5]. The photoproton data sources are ^{13}C, Ref. [15]; ^{14}C, present data; ^{17}O, Ref. [10]; ^{18}O, Ref. [5].

IV. CONCLUSION AND SUMMARY

We have reported the first measurement of the ^{14}C photoproton cross section, and have obtained an estimate of the total photoabsorption cross section for ^{14}C [the sum of the photoneutron and photoproton cross sections, with a small correction for double inclusion of (γ,pn) strength].

Essentially the entire $^{14}C(\gamma,p)$ cross section [and the $^{14}C(\gamma,pn)$ cross section, which is included above 25.71 MeV] results from decay of $T_>$ states. The $T_<$ and $T_>$ components of the ^{14}C GDR have been obtained from the available photonuclear data. The relative strengths of the two isospin components are not in good agreement with theoretical predictions. The observed splitting of the median energies of the isospin components is 8.4 ± 0.5 MeV, in agreement with predictions of Akyüz and Fallieros, and suggests a value for the symmetry potential of about 60 MeV.

Shell-model calculations of the total photoabsorption cross section for ^{14}C by Kissener *et al.* [18] and Assafiri and Morrison [19] compare well in shape and isospin distribution with experimental results. However, the placement of strength in the pygmy region relative to that in the GDR is not in good agreement with experiment; there is too little strength in the pygmy or too much in the GDR region. The $^{14}C(\gamma,p_0)^{13}B$ and $^{14}C(\gamma,n_{15.11})^{13}C$ partial cross sections predicted by Goncharova *et al.* [20] reproduce well the decay of the main $T_>$ state observed at 25.6 MeV.

This measurement completes the set of photonuclear cross sections for the carbon isotopes. Our results confirm the trends seen for other nuclei in this series of measurements. As particles or holes are added to the ^{12}C or ^{16}O core nuclei, the integrated cross section for the neutron-decay channels increases at the expense of the proton-decay channels, and the total photoabsorption cross section remains essentially constant. The addition of one, then a second, neutron to the core of ^{12}C or ^{16}O spreads the cross-section strength over an increased energy range. The behavior is similar in both the carbon and oxygen series, with the appearance of a pygmy resonance with the addition of the first valence neutron, and the gross redistribution of the absorption strength with the addition of the second valence neutron.

ACKNOWLEDGMENTS

This work was supported by grants from the University of Melbourne, the U.S. Department of Energy, and the Natural Sciences and Engineering Research Council of Canada. One of us (D.Z.) acknowledges the financial support of the University of Melbourne during part of this work. We thank Dr. H. Baer of the M.P. Division of the Los Alamos National Laboratory for arranging the loan of the ^{14}C target and helping immensely in its preparation. We are grateful to F. E. Coverdale and S. Guggenheimer for technical support, and to the members of the Betatron group for help during data taking.

[1] J. W. Jury, B. L. Berman, J. G. Woodworth, M. N. Thompson, R. E. Pywell, and K. G. McNeill, Phys. Rev. C **26**, 777 (1982).

[2] A. D. Bates, R. P. Rassool, E. A. Milne, M. N. Thompson, and K. G. McNeill, Phys. Rev. C **40**, 506 (1989).

[3] K. G. McNeill, A. D. Bates, R. P. Rassool, E. A. Milne, and M. N. Thompson, Phys. Rev. C **37**, 1403 (1988).

[4] J. W. Jury, B. L. Berman, D. D. Faul, P. Meyer, and J. G. Woodworth, Phys. Rev. C **21**, 503 (1980).

[5] J. G. Woodworth, K. G. McNeill, J. W. Jury, R. A. Alvarez, B. L. Berman, D. D. Faul, and P. Meyer, Phys. Rev. C **19**, 167 (1979).

[6] R. E. Pywell, M. N. Thompson, and B. L. Berman, Nucl. Instrum. Methods **178**, 149 (1980).

[7] J. D. Watson, J. W. Jury, P. C-K. Kuo, W. F. Davidson, N. K. Sherman, and K. G. McNeill, Phys. Rev. C **27**, 506 (1983).

[8] R. G. Johnson, B. L. Berman, K. G. McNeill, J. G. Woodworth, and J. W. Jury, Phys. Rev. C **20**, 27 (1979); J. W. Jury, J. D. Watson, D. Rowley, T. W. Phillips, and J. G. Woodworth, *ibid.* **32**, 1817 (1985).

[9] J. W. Jury, P. C-K. Kuo, K. G. McNeill, C. K. Ross, H. R. Weller, and S. Raman, Phys. Rev. C **36**, 1243 (1987).

[10] D. Zubanov, M. N. Thompson, B. L. Berman, R. E. Pywell, J. W. Jury, and K. G. McNeill, University of Melbourne Report No. UM-P-89/43, 1989.

[11] J. W. Jury, B. L. Berman, D. D. Faul, P. Meyer, K. G. McNeill, and J. G. Woodworth, Phys. Rev. C **19**, 1684 (1979).

[12] R. E. Pywell, B. L. Berman, J. G. Woodworth, J. W. Jury, K. G. McNeill, and M. N. Thompson, Phys. Rev. C **32**, 384 (1985).

[13] J. G. Woodworth, K. G. McNeill, J. W. Jury, P. D. Georgopulos, and R. G. Johnson, Can. J. Phys. **55**, 1704 (1977); Nucl. Phys. **A327**, 53 (1979).

[14] P. C-K. Kuo, K. G. McNeill, N. K. Sherman, S. Landsberger, W. F. Davidson, J. W. Jury, and R. C. Lafontain, Phys. Rev. C **31**, 318 (1985).

[15] D. Zubanov, R. A. Sutton, M. N. Thompson, and J. W. Jury, Phys. Rev. C **27**, 1957 (1983).

[16] M. C. Wright, Ph.D. thesis, Duke University, 1983; M. C. Wright, H. Kitazawa, N. R. Roberson, H. R. Weller, M. Jensen, and D. R. Tilley, Phys. Rev. C **31**, 1125 (1985).

[17] J. D. Vergados, Nucl. Phys. **A239**, 271 (1975).

[18] H. R. Kissener and R. A. Eramzhyan, Nucl. Phys. **A326**, 289 (1979).

[19] Y. I. Assafiri, Ph.D. thesis, University of Melbourne, 1984 (unpublished); Y. I. Assafiri and I. Morrison, Nucl. Phys. **A427**, 460 (1984).

[20] N. G. Goncharova, A. N. Golzov, and H. R. Kissener, Nucl. Phys. **A462**, 367 (1987).

[21] D. F. Measday, A. B. Clegg, and P. S. Fisher, Nucl. Phys. **61**, 269 (1965).

[22] S. Fallieros, B. Goulard, and R. H. Venter, Phys. Lett. **19**, 398 (1965).

[23] B. Goulard and S. Fallieros, Can. J. Phys. **45**, 3221 (1967).

[24] R. Ö. Akyüz and S. Fallieros, Phys. Rev. Lett. **27**, 1016

(1971).
[25] S. Fallieros and B. Goulard, Nucl. Phys. **A147**, 593 (1970).
[26] Evans Hayward, B. F. Gibson, and J. S. O'Connell, Phys. Rev. C **5**, 846 (1972).
[27] F. Ajzenberg-Selove, Nucl. Phys. **A449**, 1 (1986), and references therein.
[28] F. Ajzenberg-Selove, Nucl. Phys. **A433**, 1 (1985), and references therein.
[29] J. S. Pruitt and S. R. Domen, Natl. Bur. Stand. Monograph No. 48 (U.S. GPO, Washington, D.C., 1962).
[30] E. Bramanis, T. K. Deague, R. S. Hicks, R. J. Hughes, E. G. Muirhead, R. H. Sambell, and R. J. J. Stewart, Nucl. Instrum. Methods **100**, 59 (1972), and references therein.
[31] G. Kajrys, W. Del Bianco, J. Kim, S. Landsberger, R. Lecompte, S. Monaro, and P. Paradis, Can. J. Phys. **59**, 781 (1981).
[32] E. G. Fuller, Phys. Rep. **127**, 185 (1985).
[33] R. Leonardi, Phys. Rev. Lett. **28**, 836 (1972).
[34] R. R. Johnson *et al.*, Phys. Rev. Lett. **43**, 844 (1979).
[35] G. Mairle and G. J. Wagner, Nucl. Phys. **A253**, 253 (1975).
[36] V. P. Denisov, L. A. Kul'tchitskiĭ, and I. Ya. Chubukov, Yad. Fiz. **14**, 889 (1971) [Sov. J. Nucl. Phys. **14**, 497 (1972)].